JOURNAL OF PROPULSION AND POWER
Vol. 16, No. 4, July–August 2000

Numerical Investigation of Installation Effects in Turbofan Engines

W. G. Joo*
Yonsei University, Seoul 120-749, Republic of Korea

One of the important issues in the assessment of intake/engine compatibility in civil turbofan engines is the prediction of the coupling effects between the intake and the engine. An actuator-disk model has been applied to the calculations of the flow through a high-bypass-ratio turbofan geometry, including the presence of the core-support pylon and a nonaxisymmetric inlet, and the effects of the core engine. The results of a series of calculations are presented, and the nature of the interactions between the flow through a fan and the system components is addressed.

Nomenclature

$\boldsymbol{A}$	= area vector of the control volume surface
C_p, C_V	= specific heat
E	= total internal energy, $c_V T + V^2/2$
H	= total enthalpy
$\boldsymbol{i}_x$, $\boldsymbol{i}_\theta$, $\boldsymbol{i}_r$	= unit vectors in r, θ, and x directions
$\dot{m}$	= mass flow rate
P_0	= total pressure
p	= pressure
T_0	= total temperature
t	= time
$\boldsymbol{V}$	= absolute velocity
$\boldsymbol{V}_x$, $\boldsymbol{V}_\theta$, $\boldsymbol{V}_r$	= velocity components in r, θ, and x directions
ρ	= density
$\bar{\bar{\tau}}$	= stress tensor containing both the static pressure and viscous stresses
Ω	= volume of the control volume

Subscripts

x, θ, r	= axial, tangential, and radial directions

Superscript

$-$	= mass averaged at dadius

I. Introduction

THE design of the intake for modern turbofan engine installations traditionally and to a large extent still takes place independently of that of the engine. The acceptability of the intake design is usually determined by experiments performed on the intake alone. However, when the engine is installed in its intake, the performances of the intake and the fan can be very different from those measured in isolation. This is largely caused by the coupling between the flowfield delivered by the intake and that of the engine.

The intake of a civil high-bypass-ratio turbofan engine (Fig. 1) is usually drooped relative to the engine centerline, typically, at approximately 6 deg, to align the intake more fully with the oncoming flow, which has a positive vertical component induced ahead of the wing. In addition, the intake is usually asymmetric, with a thicker lower lip to allow for the inlet being subjected to positive incidence at various parts of the takeoff and climb. Even though the flow delivered to a fan is a uniform stagnation pressure flow, a nonuniform static pressure field is produced at the fan face by the asymmetric nature of such a drooped nonaxisymmetric intake.

In addition, there is usually a large pylon, which supports the weight (and carries various engine services), and at least one other strut, which provides some rigidity for the engine structure. These support structures for the core and rotating assemblies of a modern turbofan engine present a considerable blockage for the bypass section and subject the fan to a nonuniform back pressure. This nonuniform static pressure field upstream and downstream of the fan affects the performance and the stability of the fan, and it is a matter of some concern to manufacturers. Despite the importance of the problem, however, few prediction methods or empirical correlations have been reported for the flow through a fan that take into account the interaction with the inlet and with the pylon.

For the calculation of nonuniform flow, the whole blade passage in the annulus must be included in the calculation domain, but this calculation, which requires large CPU time and large memory, is not practical at the design stage. This leads to the need to model the flow within the blade rows, and various blade row models could be considered for this purpose. Joo and Hynes[1] argued that actuator-disk models of blade rows are an appropriate approximation because the nonuniformities of static pressure due to the droop and due to the presence of the pylon have a length scale of the order of the circumference, and they[1] developed a three-dimensional computational method using actuator-disk models of blade rows for the calculation of nonuniform flow with a long length scale.

This paper presents the results of a series of calculations performed for a typical modern high-bypass turbofan engine using the method developed by Joo and Hynes[1] and discusses the nature of the interaction between the flow through a fan and through system components.

II. Calculation Method

A. Calculation Domain

Figure 2 shows a cross section of the calculation domain that is used to model the flow through the engine and its installation. The engine has a droop simulator designed for taking into account the effect of a drooped intake at cruise.

A fan and an outlet guide vane (OGV) in the bypass duct are contracted to plane actuator disks, which are located at the midchord of each blade row. The flowfields upstream and downstream of the blade row are found using a fully three-dimensional computational method and are coupled by boundary conditions imposed across the actuator disk to represent the blade row performance. The locations of the OGV actuator disk and the splitter are moved slightly toward the fan to keep the true actual gap distances between them and the fan.

It is necessary to simulate all components of the engine downstream of the fan that are thought to affect the response of the fan.

Received 28 November 1998; revision received 23 March 1999; accepted for publication 29 March 1999.

*Assistant Professor, Department of Mechanical Engineering, 134 Shinchon-dong, Sudaemun-ku. Member AIAA.

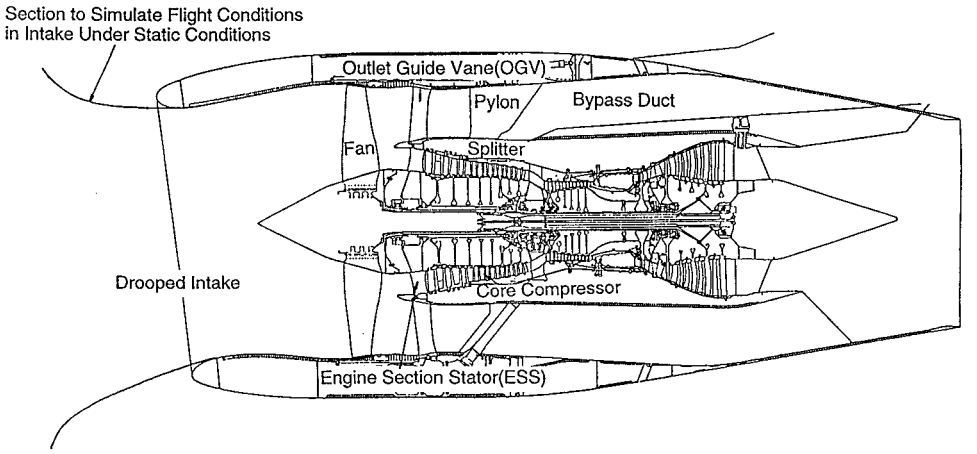

Fig. 1 Schematic of typical turbofan engine with inlet simulator.

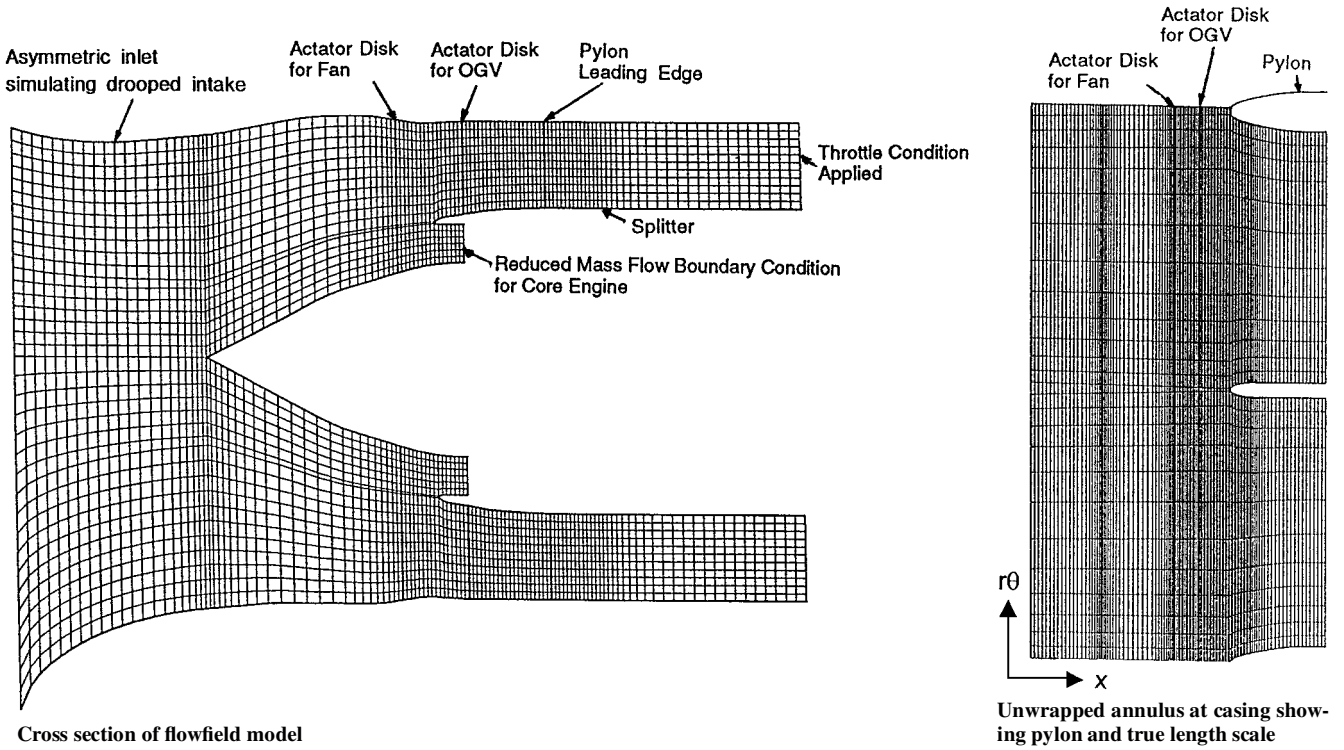

Cross section of flowfield model

Unwrapped annulus at casing showing pylon and true length scale

Fig. 2 Calculation grids used for predictions of fan/OGV/pylon flowfield interactions.

The flowfield downstream is split into core and bypass streams. The calculation domain in the core engine section is extended to just upstream of the engine section stator (ESS), where a boundary condition simulating the presence of the core engine is imposed. The calculation domain in the bypass stream is continued around the pylon and the corresponding strut at bottom dead center to a section well past the pylon leading edge.

General details of the computational method using actuator-disk blade row models and the important issues related to an actuator-disk model, such as the sensitivity of solution to the disk location, are described by Joo and Hynes,[1,2] and thus, only a brief description of the method and the extra details relevant to the current calculation are given here.

B. Computational Method for Flowfield Regions

The flowfields upstream of the fan, between the fan and OGV, and downstream of the OGV, shown in Fig. 2, are found from the solutions of three-dimensional Reynolds averaged Navier–Stokes equations in conservation form. These equations are written in the absolute frame using a cylindrical coordinate system because the distorted flowfield is assumed to be steady in this frame; thus,

$$\frac{\partial}{\partial t}\int_{\Omega} U\,\mathrm{d}\Omega + \int_{A} \boldsymbol{F}\cdot\mathrm{d}\boldsymbol{A} = \int_{\Omega} Q\,\mathrm{d}\Omega$$

where

$$U = \begin{bmatrix} \rho \\ \rho V_x \\ \rho V_\theta \\ \rho V_r \\ \rho E \end{bmatrix}, \qquad \boldsymbol{F} = \begin{bmatrix} \rho \boldsymbol{V} \\ \rho V_x \boldsymbol{V} + \overline{\overline{\tau}}\boldsymbol{i}_x \\ r\rho V_\theta \boldsymbol{V} + r\,\overline{\overline{\tau}}\boldsymbol{i}_\theta \\ \rho V_r \boldsymbol{V} + \overline{\overline{\tau}}\boldsymbol{i}_r \\ \rho H \boldsymbol{V} \end{bmatrix}, \qquad Q = \begin{bmatrix} 0 \\ 0 \\ 0 \\ \dfrac{\rho V_\theta^2 + p}{r} \\ 0 \end{bmatrix}$$

These equations are discretized on a set of control volumes, formed by a simple, structured H-grid construction. Flow variables are stored at cell centers, and values on cell faces for flux evaluation

are, thus, found by a simple average of the cell variables on either side of the face with second-order accuracy on smoothly varying grids.

There are potential problems raised by the singular points at zero radius in a cylindrical coordinate system, but these singular points pose few problems for cell-centered finite volume methods because flow variables need not be defined there. Only the evaluation of fluxes through the face located at zero radius is required to solve the discretized equations of motion. These fluxes are set to zero because the face area is zero.

The size of the grids near the boundaries used for the calculation is too large in comparison with a boundary-layer thickness to resolve annulus boundary layers. Therefore, only the laminar shear stress, not turbulence, is considered, and the calculation effectively would become an inviscid one. The discretized set of equations of motion are solved by time marching. The basic solution algorithm is the same as that developed by Dawes[3] for the calculation of the flow within a single blade row passage. This time marching scheme consists of a two-step explicit and one-step implicit scheme derived as a preprocessed simplification of the Beam–Warming algorithm.

The flow at the inlet boundary to the calculation domain is assumed to be nonswirling, to have uniform stagnation pressure and stagnation temperature, and to be roughly aligned with the streamwise surfaces of the calculation grid.

At the outlet boundary located just upstream of the ESS in the core engine section, a condition simulating the presence of the core engine is imposed. The pressure rise characteristics of the core engine are very steep when compared with those of the fan root, and thus the core compressor will not accept much in the way of a circumferentially nonuniform reduced mass flow. A constant mass flow coefficient, $\dot{m}\sqrt{(C_p T_0)}/AP_0$, therefore, is specified at each radius and circumferential position.

The outlet boundary in the bypass section is located at some distance downstream of the pylon leading edge and the corresponding strut leading edge at the bottom. If the flow at the outlet to the calculation domain is assumed to have no circumferential variation, the imposed boundary condition is usually the fixed hub or tip static pressure, with the radial variation consistent with simple radial equilibrium. This is a good approximation for blade to blade calculations where the only circumferential static pressure variation present has a length scale of at most one blade pitch and variations that are made up of such high order that circumferential harmonics decay axially in a short distance. Any interaction of these static pressure variations with the downstream boundary usually has a negligible effect on the flow in the blade row.

However, the static pressure variations present in the flow with strong flowfield interaction have considerable low-order circumferential harmonics, which persist a long way downstream, and thus radial equilibrium is not appropriate as an outlet boundary condition. Its imposition, even at some far distant downstream location, caused considerable problems with numerical convergence to a steady solution.

Joo and Hynes[1] suggested a simple, new approach to handle such a complicated boundary condition. The calculation domain is imagined to be terminated at the downstream end by a gauze honeycomb. This was chosen because a gauze honeycomb is an almost realizable device that will turn the flow at each radial and circumferential position to the axial direction. The static pressure downstream of the honeycomb will, thus, be uniform. The gauze honeycomb also has throttlelike pressure drop characteristics, and this might be expected to have a benign effect on the transient aspect of the convergence process. The presence of such a device will, of course, affect the flow upstream of the outlet boundary, so that the outlet boundary should still extend to a sufficient length downstream of the fan to ensure that the flow through the rotor itself is not affected. A detailed description of the implementation of this outlet boundary condition into a numerical scheme is found in Ref. 1.

C. Actuator-Disk Boundary Conditions

The length scales that characterize the flow interactions between fans and intakes and the downstream components are likely to be much larger than a blade pitch. In addition, it will be seen that some of the compatibility issues do not directly involve the flow within the blade rows. In these circumstances, an actuator-disk model for a blade row would seem a useful first approximation.

The flowfields upstream and downstream of the blade row are coupled by boundary conditions imposed across the actuator disk to represent the fan performance. Five matching conditions are required across an actuator disk, corresponding to the five independent flow variables in the equations of motion. The boundary conditions used in the present model, which are applied at each radial location and at each circumferential position, are: 1) conservation of mass, 2) conservation of radial momentum, 3) conservation of rothalpy, 4) relative exit flow angle specified, and 5) entropy rise (or total pressure change) specified.

The last two conditions are associated with blade performance, which are given as input data. The flow angle at the exit to the actuator disk could be taken directly from the values of the measured or calculated flow angle at the blade trailing edge. In the present calculations, the values of the relative flow angles and losses at the exit to the fan actuator disk were obtained from a three-dimensional viscous calculation (using BTOB3D) of the flow through the fan operating near design in a uniform inlet flow. The radius of the annulus varies significantly through the fan blade row, as shown in Fig. 1. The work done by the fan disk, therefore, is influenced somewhat by the disk location if the true blade exit flow angles are used. To reproduce the correct work distribution, the true flow angles are corrected slightly using an approximate method suggested by Joo and Hynes.[1] The OGV is assumed to turn the flow to the axial direction without deviation. The flow through the rotor subjected to the nonuniform inlet flow is unsteady to a certain extent, but this unsteady effect is assumed to be neglected.

Conditions 1–5 just described must be modified when blade sections are choked because this set of boundary conditions does not contain an allowance for blade blockage. In the present calculations, a simple model for choking, suggested by Joo and Hynes,[1] based on two-dimensional flow into a choked blade section, was incorporated into the actuator-disk boundary conditions 1 and 5.

The way to integrate these actuator-disk boundary conditions into a numerical model depends on the numerical scheme used for calculating flowfield regions. Detailed implementation of actuator-disk boundary conditions used in the present calculation may be found in Ref. 1.

III. Calculation Results

The calculations are performed for an engine operating at 95% of design fan speed, where the total pressure ratio is about 1.68, the mass flow is 916 kg/s, and the bypass ratio is 4.51. A $27 \times 121 \times 19$ finite volume grid is used. Computations reach an acceptable level of convergence at approximately 2000 time steps corresponding to 240 min of CPU time with an IBM RISC 6000/350.

The calculation results are compared with the total pressure measured using a number of rakes mounted near the leading edge of the OGV and ESS in Fig. 3, which was also presented by Joo and Hynes,[2] for the validation of the present computational methods. Because our major interest is the circumferential asymmetry in the flow, the values shown in Fig. 3 are percentage variations about the mean representing the average value at that particular radius,

$$\frac{P_0(r,\theta) - \overline{P_0}(r)}{\overline{P_0}(r)} \times 100\,(\%)$$

Figure 3 shows that the calculation results are in good agreement with the experimental data for both the level and the pattern of the variation. The major difference between the two results is in the angular position; the predicted flowfield is shifted by about 30 deg in the direction opposite to fan rotation relative to the measurements. The neglect of unsteadiness, which causes the time lag response of the fan, in framing the rotor actuator-disk boundary conditions is a possible reason for the difference, as is the modeling of the entire core section of the engine by a boundary condition. The shift in angular position is also due to the actuator-disk model with zero

length that cannot consider a particle path within a blade passage. This is the only comparison with experimental data for validation of the method because the experimental data available are limited, but the agreement between the calculated and the measured results in Fig. 3 is sufficient for many engineering purposes. The flowfield immediately downstream of the fan and, by inference, the flowfield immediately upstream are probably accurate enough, for example, to enable realistic estimates of the circumferential variation in loading on rotor blades to be made for the purposes of fan vibration and noise-level assessments.

Both sets of results show that the total pressure delivered by the fan has an 11% variation about the mean value around the annulus at the tip and 8% variation at the hub. This asymmetry of total pressure rise is caused by the effects of nonaxisymmetric inlet geometry combined with the upstream effects of the core engine and the pylon. Therefore, a series of calculations was performed to identify the magnitude of the effect of each component on the fan performance.

IV. Drooped Intake/Fan Flowfield Interaction

To investigate the characteristics of drooped intake and fan flowfield interaction, calculations have been performed for the drooped intake and fan flowfields where all components downstream of the fan are removed. In addition, the calculation for the duct alone with no fan present was performed to see the upstream flow redistribution due to the presence of the fan. In the both calculations, the throttlelike boundary condition is applied at the outlet boundary to the calculation domain. The throttle coefficient for the calculation of the duct alone was set to give the same mass flow as the one for the calculation of the drooped intake with the fan.

The percentage variation of static pressure at the fan actuator-disk inlet is shown in Fig. 4 for both calculations. The calculation of

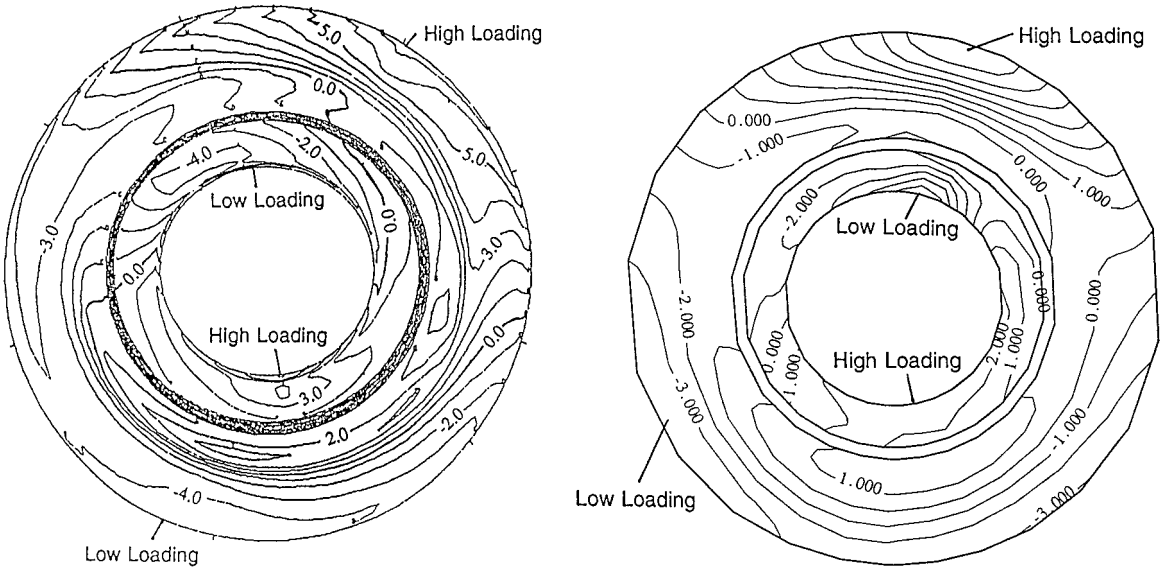

Experiment **Prediction**

Fig. 3 Comparison of measured and predicted variations (%) of total pressure near OGV inlet.

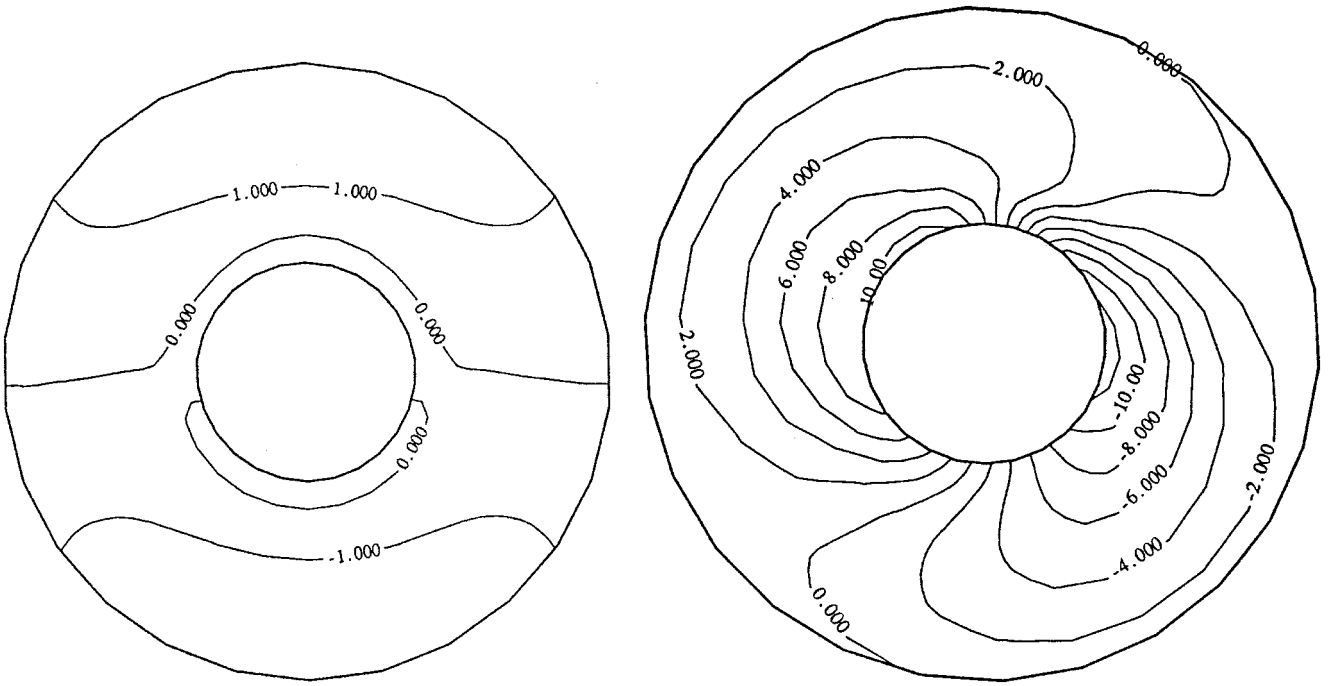

Without fan **With fan**

Fig. 4 Comparison of predicted variation (%) of static pressure at fan actuator-disk face for drooped inlet with and without the presence of a fan.

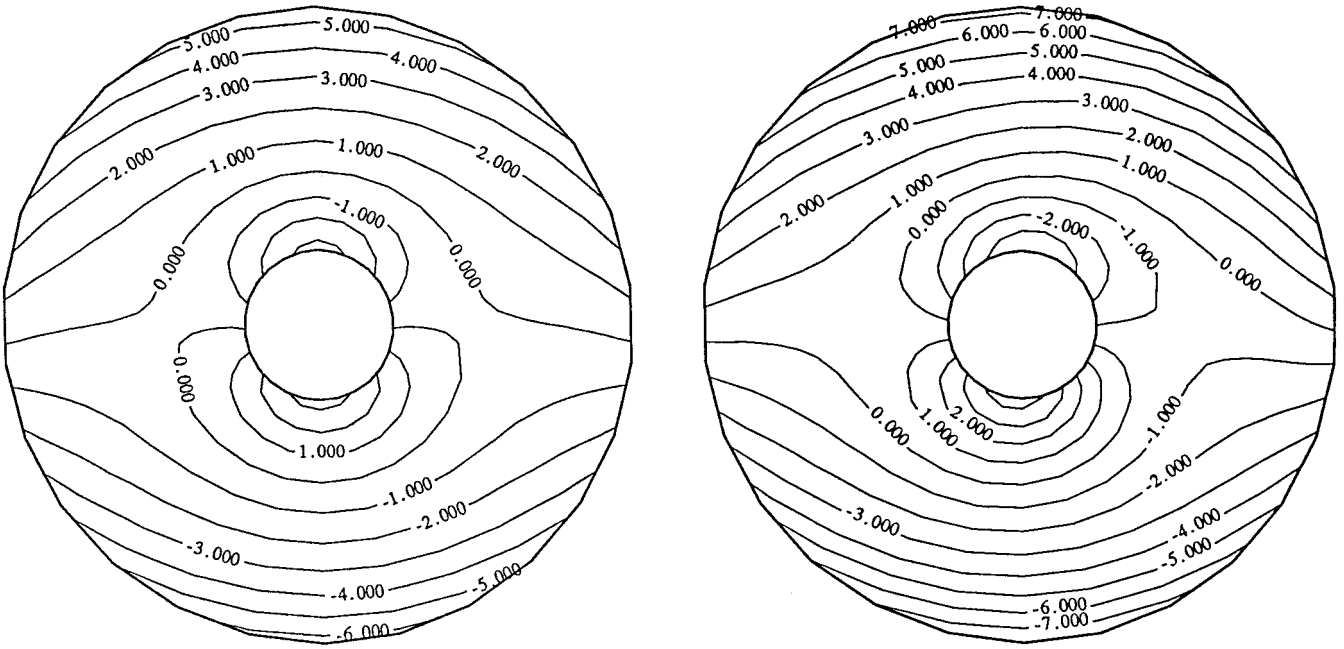

Without fan **With fan**

Fig. 5 Comparison of predicted variation (%) of static pressure at half mean radius upstream of fan actuator disk for drooped inlet with and without the presence of a fan.

the duct without the fan shows the symmetric and small static pressure variation. This shows that the large-scale nonuniform static pressure field produced by the asymmetric drooped intake becomes uniform as the annulus becomes axisymmetric. On the other hand, the presence of the fan considerably modifies the static pressure field upstream of the fan for both the level and phase of the variation. The circumferential position of the peak value is rotated by about 45 deg in the direction opposite to fan rotation, and the level of nonuniformity is much higher. The effect on the upstream flow redistribution appears more strongly in the hub region than in the tip region. The strength of this effect decays upstream of the fan and is negligible at half a mean radius upstream (Fig. 5).

The static pressure variation at the fan face must be accompanied by variations in axial and circumferential velocity because total pressure is uniform upstream of the fan. The resulting changes in flow coefficient and in incidence will produce nonuniform fan performance at each circumferential and radial position. The percentage variation of the total pressure at the fan actuator-disk exit is shown in Fig. 6. The result indicates that the effect of the drooped intake on the fan performance is stronger in the hub region (7% variation) than in the tip region (4% variation).

When compared with the prediction including the combined effects of all components (Fig. 7), it can be seen that the asymmetry of the fan performance is similar in the core section, whereas in the bypass section, the total pressure variation due to the drooped intake is small, particularly in the top region. This suggests that the effect of the drooped intake dominates the change of fan performance in the core section, but other components have a stronger effect on the flow in the bypass section.

V. Core Engine/Fan Flowfield Interaction

When operating in circumferentially nonuniform flow, a compressor generates a nonuniform static pressure field upstream to match upstream and downstream flowfields across the compressor.[4] Hence, the core compressor can be coupled with the nonuniform flow that is delivered by the fan and the compressor produces a nonuniform static pressure field upstream. This static pressure distortion decays upstream of the core compressor, but it is still possible to significantly affect the fan exit flow condition.

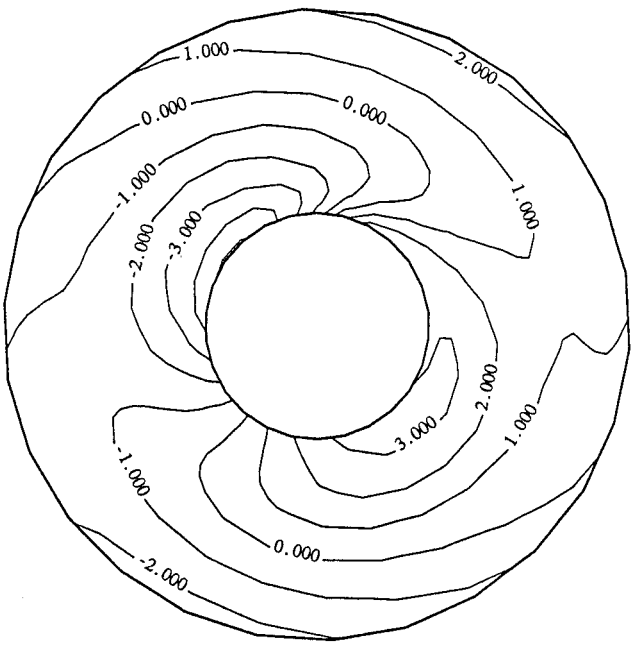

Fig. 6 Predicted variation (%) of total pressure at the exit of a fan operating behind a droop inlet without all downstream components.

To investigate this effect of the core compressor, a calculation was performed for the fan with the drooped intake and the core engine but with no pylon. The predicted fan performance is compared with that without the core compressor in Fig. 8. As one might expect, the presence of the core engine does reduce the asymmetry of the flow produced by the fan in the hub region, but the effect on fan performance is relatively small near the design operating condition.

An important factor that may strongly affect the strength of flowfield interaction between the fan and the core compressor is the bypass ratio.[5] At design, the bypass ratio is usually similar to the effective bypass ratio for the isolated fan, which is defined by the streamline that passed through the position occupied by the leading

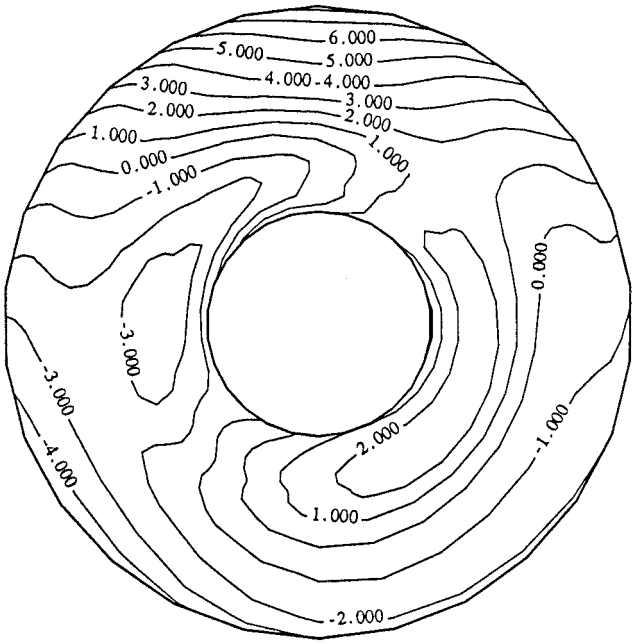

Fig. 7 Predicted variation (%) of total pressure at the exit of a fan operating behind a droop inlet with all downstream components.

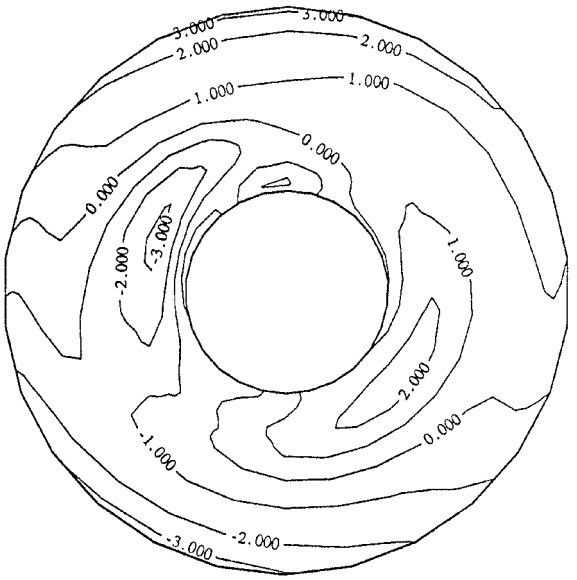

Fig. 8 Predicted variation (%) of total pressure at the exit of fan operating behind a droop inlet with core engine and no pylon.

edge of the splitter. Therefore, the change in bypass ratio due to the presence of the core is usually very small.

Near stall, however, the core engine, which usually has very steep pressure rise characteristics, will not accept much of a variation in reduced mass flow, so that more flow moves into the core stream. As a result, the bypass ratio will be lower than the effective bypass ratio, and the flow in the core region is always accelerating. As bypass ratio is reduced, the stabilization of the fan is stronger due to the interaction with the core compressor, as observed by Lambie.[5] The investigation of the effect of changing the bypass ratio is suggested for future work.

VI. Pylon/Fan Flowfield Interaction

The pylon represents a considerable blockage to the bypass stream and generates large static pressure disturbances associated with the low harmonics of long length scale. Its effect can be felt a long way upstream and will still be significant at the fan exit. A view of the grid in an axial–circumferential sense in the vicinity of the casing is shown in Fig. 2, where the grid is drawn with equal scales for axial and circumferential distances to show just how close (in aerodynamic terms) are the fan, the OGV blade rows, and the struts.

To investigate the effects of the pylon only in the bypass stream section, the effect of the drooped intake is eliminated by the use of an axisymmetric inlet. The percentage variation of total pressure at the fan actuator disk exit is shown in Fig. 9. The pylon effect on fan performance is almost symmetric and greatest in the top region. Note that this pylon effect is not restricted to the bypass region; it also appears in the core region. This is clearly the result of the radial redistribution of the flow, which cannot be predicted using two-dimensional analysis. When this is compared with the results that include the effects of the drooped intake in Fig. 7, it can be seen that the fan performance in the top region is primarily influenced by the presence of the pylon.

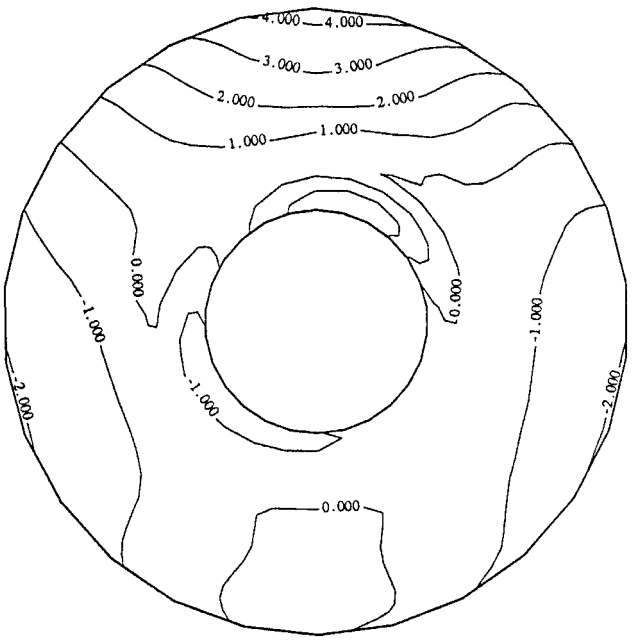

Fig. 9 Predicted variation (%) of total pressure at the exit of a fan operating behind an axisymmetric inlet with all downstream components.

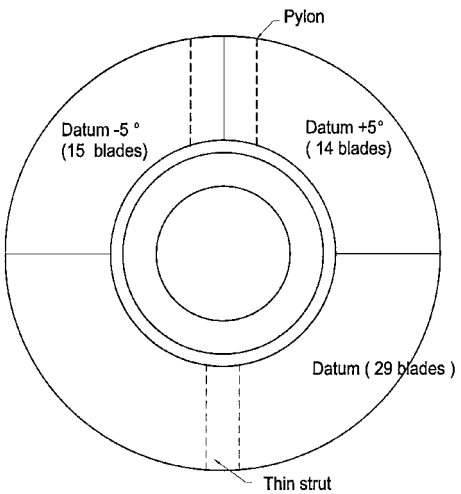

Fig. 10 Typical cyclic pattern of blade angles at the OGV exit for blocking the pylon effects.

The OGV between the fan and the pylon can significantly affect the characteristics of the upstream propagation of a static pressure disturbance. Chiang and Turner[6] demonstrated that the magnitude of static pressure perturbation propagating across the OGV is a function of the inlet and exit angles of the OGV by modeling the vane as an actuator disk. Therefore, modern turbofans often use a nonaxisymmetric set of OGVs to ameliorate the upstream effect of the pylon blockage.

Figure 10 shows the typical pattern of blade angles at the OGV exit designed to block the pylon effects. To fully block the pylon effects, more blades with different exit angles should be used, but this cyclic OGV consists of only three types of exit blade angles to reduce cost. Using the present method, an investigation is made of how much this type of cyclic OGV can block the pylon effects. To calculate for cyclic OGV, the nonuniform set of OGV exit flow angles is simply specified as an OGV actuator-disk boundary condition for the exit flow angles.

Figure 11 shows the comparison of static pressure variations predicted at the OGV inlet for uniform and cyclic OGVs. The static pressure variation at the uniform OGV exit is about 9% of the mean value near the casing, whereas the variation at the cyclic OGV exit is about 4%. As the static pressure variation is reduced, the variation of total pressure rises by the fan will be reduced. Figure 12 shows the total pressure variations predicted at the OGV inlet for uniform and cyclic OGVs. The total pressure variation at the uniform OGV exit is about 8% of the mean value near the casing, whereas the variation at the cyclic OGV exit is about 3%. The static and total pressure variations in the circumferential direction at the casing, midspan of OGV, and at the hub of a core engine are shown in Figs. 13 and 14, respectively. It can be seen that a large reduction in the circumferential variation of the static and the total pressure occurs at the position of pylon. The calculations suggest that this type of cyclic OGV can reduce the propagated variations by half as compared to the uniform OGV.

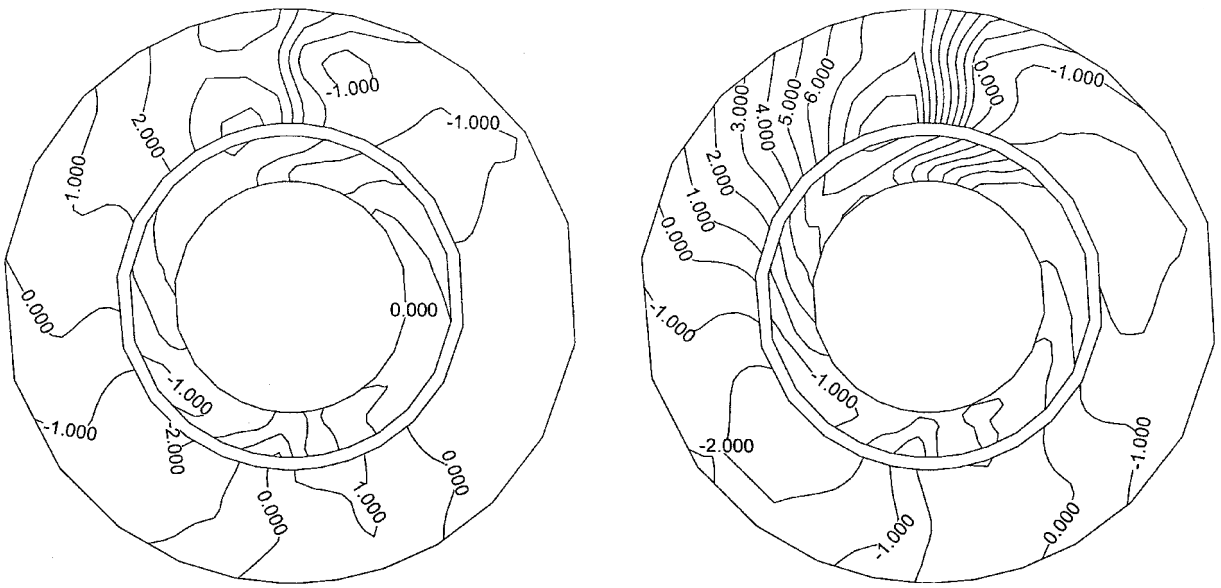

Cyclic OGV **Uniform OGV**

Fig. 11 Comparison of predicted variation (%) of static pressure at the OGV inlet for uniform and cyclic OGVs with an axisymmetric inlet.

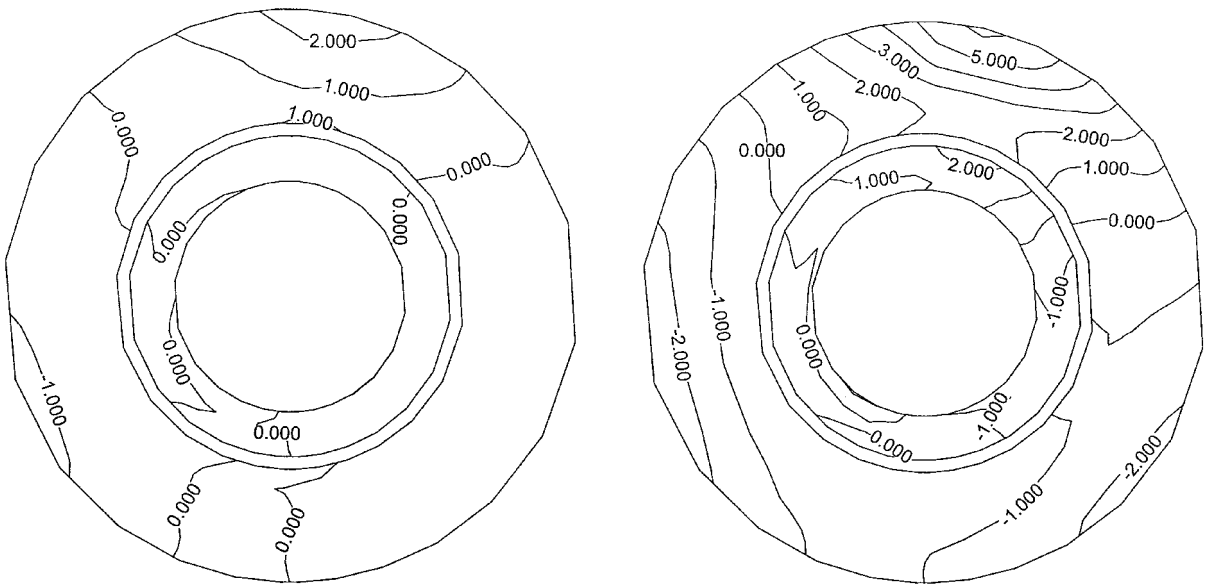

Cyclic OGV **Uniform OGV**

Fig. 12 Comparison of predicted variation (%) of total pressure at the OGV inlet for uniform and cyclic OGVs with an axisymmetric inlet.

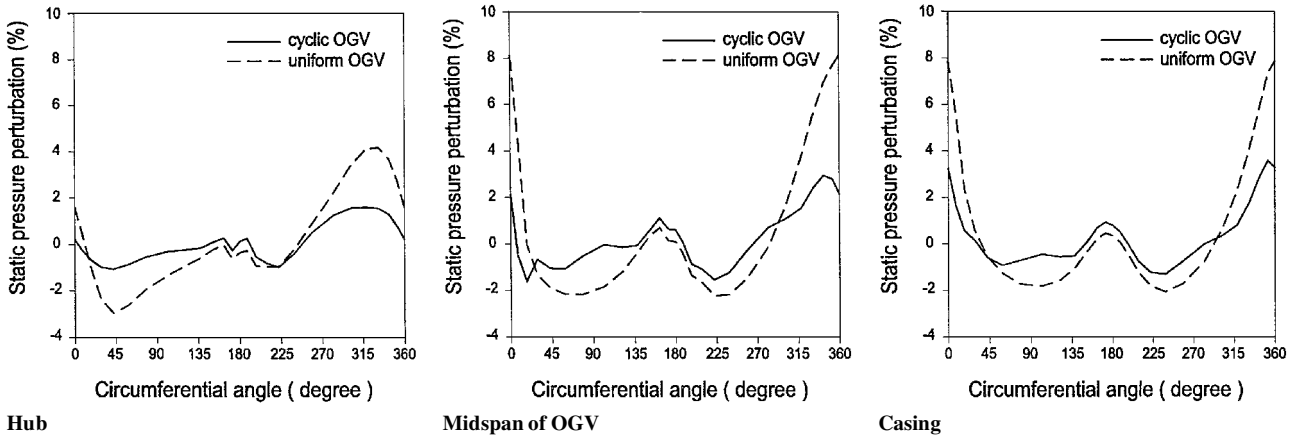

Fig. 13 Comparison of predicted variation (%) of total pressure in the circumferential direction for uniform and cyclic OGVs with an axisymmetric inlet.

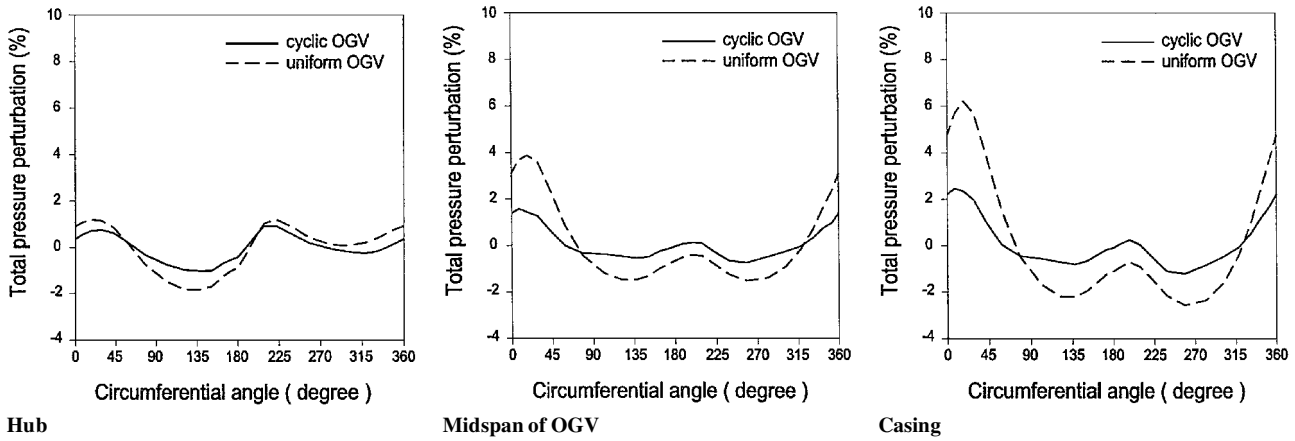

Fig. 14 Comparison of predicted variation (%) of total pressure in the circumferential direction for uniform and cyclic OGVs with an axisymmetric inlet.

VII. Conclusions

One of the important issues in the assessment of intake/engine compatibility in civil turbofan engines is the prediction of the coupling effects between the intake and the engine. An actuator-disk model has been applied to the calculation of the flow through a high-bypass-ratio turbofan geometry including the effects of the presence of the core support pylon, the core engine, and a nonaxisymmetric inlet.

The upstream flowfield is significantly redistributed by the interaction between the engine and nonuniform inlet static pressure due to the drooped intake. The axial scale over which the upstream flow redistribution takes place is about half a mean radius.

The asymmetry in the flow through a modern turbofan is mainly attributed to the drooped intake and to the pylon, and the effect of the core compressor is relatively small near the design operating condition. The pylon has a stronger effect than the drooped intake in the bypass stream section, whereas the droop effect is more important in the core engine section. It appears that the two effects have similar phasing, which unfortunately implies a purely additive effect. In addition, estimates of the asymmetric flow entering the core section of the engine indicate that the levels of asymmetry there are likely to be almost as high as in the bypass section of the engine.

The effects of a pylon can be blocked by the circumferential nonuniform distribution of OGV exit blade angles. The calculation shows that about half of the nonuniformity propagated through the uniform OGV can be blocked by the use of the cyclic OGV, which has a simple pattern of three types of blades with different exit angles.

Acknowledgments

The author thanks T. P. Hynes at the Whittle Laboratory, University of Cambridge, for his invaluable advice and help in this work. He is also grateful for the support provided by N. T. Birch at Rolls–Royce, plc.

References

[1] Joo, W. G., and Hynes, T. P., "The Simulation of Turbomachinery Blade Rows in Asymmetric Flow Using Actuator Disks," *Journal of Turbomachinery*, Vol. 119, No. 4, 1997, pp. 723–732.

[2] Joo, W. G., and Hynes, T. P., "The Applications of Actuator Disks to Calculations of the Flow in Turbofan Installations," *Journal of Turbomachinery*, Vol. 119, No. 4, 1997, pp. 733–741.

[3] Dawes, W. N., "Development of a 3D Navier–Stokes Solver for Application to All Types of Turbomachinery," American Society of Mechanical Engineers Paper 88-GT-70, 1988.

[4] Longley, J. P., and Hynes, T. P., "Stability of Flow Through Mutistage Axial Compressors," *Journal of Turbomachinery*, Vol. 112, No. 1, 1990, pp. 126–132.

[5] Lambie, D., "Inlet Distortion and Turbofan Engines," Ph.D. Thesis, Dept. of Engineering, Univ. of Cambridge, Cambridge, England, UK, 1989.

[6] Chiang, H.-W. D., and Turner, M. G., "Compressor Blade Forced Response due to Downstream Vane-Strut Potential Interaction," *Journal of Turbomachinery*, Vol. 118, No. 1, 1996, pp. 134–142.